OPTICS and LASERS in ENGINEERING

ELSEVIER Optics and Lasers in Engineering 31 (1999) 247–261

A high-speed all-digital technique for cycle-resolved 2-D flow measurement and flow visualisation within SI engine cylinders

M. Reeves[a,*], D.P. Towers[b], B. Tavender[b], C.H. Buckberry[b]

[a]*Scitek Consultants Ltd, Sunnylea, 157 Burton Road, Derby DE23 6AB, UK*
[b]*Rover Group, Applied Optics Laboratory, Bld 102A, Gaydon Test Centre, Warwickshire CV35 0RG, UK*

Received 21 December 1998; received in revised form 20 July 1999; accepted 21 July 1999

Abstract

Particle image velocimetry (PIV) is now a well-established planar flow measurement technique for the study of in-cylinder flow fields in internal combustion engines. Here the authors describe a turnkey, high-speed digital imaging system that provides combined real-time flow visualisation and rapidly processed PIV data in an industrial optical research engine facility. The system is based on commercially available, high-speed imaging and laser technology and conventional digital cross-correlation processing to provide cycle-resolved PIV data and flow visualisation within timescales appropriate for engine development. A simple variation on the synchronisation scheme also allows the acquisition of tens to thousands of flow visualisation sequences and PIV maps at the same crank angle, thus giving the potential for the study of cycle-to-cycle flow variability and its effect on combustion stability in a suitably instrumented optical engine. The technique may also find applications in other unsteady or oscillatory flows of importance in aerodynamics, acoustics, mixing, and heat transfer.

Keywords: Particle image velocimetry; PIV; Digital; Internal combustion engine; Cycle-resolved; High-speed imaging

* Corresponding author. Tel./Fax: + 44 (0)1332-748247.
E-mail addresses: mark.reeves@scitekconsultants.co.uk (M. Reeves), david.towers@compuserve.com (D.P. Towers)

0143-8166/99/$ - see front matter
PII: S0143-8166(99)00026-3

1. Introduction

1.1. Motivation

Fluid motion within IC engines is known to fundamentally affect IC engine performance and emissions [1,2]. The flow inside engine cylinders is of a turbulent nature and also exhibits large- and small-scale cyclic variations. The nature of the large-scale flow structure, turbulence characteristics and cyclic variability are known to impact profoundly on engine performance. Hence whole field techniques such as particle tracking velocimetry (PTV) [3–5] and particle image velocimetry (PIV) [6,7] are finding increasing application in the study of in-cylinder flows. These closely related techniques are capable of providing instantaneous snapshots of unsteady velocity fields and are reviewed in Ref. [8]. Particle image velocimetry, although computationally intensive, relies on simple and generic spatial correlation techniques to determine the mean particle velocity within each of many small regions in the flow, and it is this analysis technique which has been used in this work.

IC engine-related PIV studies to-date have included the measurement of: motored [6] and fired [9] flows in high axial swirl engines; intake flow past inlet valves [10]; and cylinder wall ported engine flows under motored and fired conditions [11]. The tumbling flow within vertical planes have also been characterised in a motored four-valve engine [12].

The area-bandwidth product of the imaging medium (i.e. the total number of resolvable picture elements available to record the particle image fields) and the nature of the interrogation procedure dictate the trade-off between the measurement field of view, spatial resolution and velocity accuracy in a given PIV experiment. Examples of the measurement performance achievable using a variety of image sensors and optics are discussed in [13]. To record PIV data over a typical in-cylinder field of $\sim 80 \times 80$ mm and at a spatial resolution and accuracy suitable for small-scale turbulence studies requires high-resolution photographic film recording and, wherever possible, cross-correlation analysis in order to resolve directional ambiguity (e.g. [14]). This permits the resolution of small-scale turbulence required for fundamental studies of the interactions between the turbulent in-cylinder flow field and flame propagation. Although many PIV practitioners prefer exclusively digital imaging with its on-line optimisation capability and convenience, it has been shown that with careful attention to experimental detail, photographic PIV techniques can be applied routinely with good success rates [15].

While the photographic techniques provide the most detailed velocity data over the widest possible areas, the difficulties in high-speed film transport and the time from experimentation to the presentation of velocity data may present a significant obstacle to the use of photographic PIV in industrial engine development programs, particularly if statistically significant cyclic variability data or cycle-resolved time series of vector fields are required.

The ability to resolve fine flow detail is, however, not necessarily required in all measurement cases. For example, the study of filling flows during the induction stroke and the more important large scale flow patterns generated after the time of inlet valve closure during compression require only moderate spatial resolution and velocity accuracy for their characterisation. In these cases, high frame rate digital imaging and PIV processing can provide data on a timescale appropriate to engine development needs.

An all-digital PIV system for in-cylinder flows based on cross-correlation of the odd and even fields of a standard CCD camera is described in [16]. This was capable of recording PIV snapshots at a selected crank angle for the convenient study of statistical flow variations, but the frame rate did not permit a cycle-resolved PIV time series to be generated. In another study, a 2000 frames/second CCD camera system combined with a light sheet scanned in the direction of its normal permitted the estimation of 3 velocity components in an in-cylinder engine flow [17]. However, the scanning mechanism and the need to temporally track correlation peaks from one plane to the next strongly compromised crank angle resolution in return for a limited ability to reconstruct three-dimensional flow fields.

The requirements of the authors' system were to provide cycle-resolved PIV data and flow visualisation to characterise the evolution of the in-cylinder flow within individual engine cycles, with a crank angle resolution of the order of 1°CA at a typical engine speed of 1500 RPM. In addition, a large number of successive engine cycles were to be analysed at a given crank angle to assess cyclic variability. A spatial resolution of 5 mm and a velocity dynamic range of 15 : 1 was considered appropriate, with an overall velocity accuracy of the order of $\pm 10\%$. The seed particles were required to give high contrast point-like particle images with moderate pulse illumination energy, and yet follow turbulent fluctuations of up to 1 kHz at an amplitude accuracy of better than 95%. The spatial resolution and accuracy requirements are much less strict than those expected in high resolution PIV experiments. However, the challenge was to minimise the time taken from experimentation to data presentation: less than 3 weeks for 4 light sheet positions $\times$ 3 engine parameters, plus cyclic variability sequences at a single light sheet position $\times$ 3 engine parameters $\times$ 2 crank angles.

1.2. Particle image velocimetry

PIV is now a well established technique for the measurement of instantaneous planar velocity fields and has been reviewed by a number of authors [8,18]. In its simplest form, the flow is illuminated with a double pulsed light sheet and the positions of tracer particles are recorded with a photographic camera viewing normal to the plane of the sheet. The mean particle displacement vector in each small region of the flow is determined by performing a spatial correlation of the particle image field in that region. If the image is a simple double-exposure then autocorrelation analysis is used. If the first and second particle image fields can be recorded separately, the more robust cross-correlation interrogation methods may be used [19]. This gives the important benefits of improved measurement dynamic range, better tolerance to velocity gradients and seed concentration variations and elimination of directional ambiguity. The photographic recording of high-speed time series of moving particle fields for cross-correlation PIV has been reported for combustion studies in constant volume vessels [20] and also in cycle-resolved engine studies [21].

It has been shown by practitioners of digital PIV that, depending on details of the flow structure, reasonable accuracies may be achieved using interrogation region dimensions as low as 16×16 pixels, with the condition that particle images occupy no less than 2×2 pixels [22,23]. Thus, the possibility exists of generating velocity measurements on a regular grid of 16×16 locations with a 50% overlap, each calculated using an FFT-based cross-correlation of 16×16 pixel interrogation region, over an image field of 128×128 pixels. This resolution is adequate for the characterisation of large-scale flow structures encountered in typical IC engines after inlet valve closure and before the rapid flow distortion that may be encountered in the last stages of compression. The available resolution may be used to study a large region with a relatively sparse measurement grid, or a PIV probe system could alternatively be used to measure flow in smaller regions to higher spatial resolution or accuracy.

2. Experimental

2.1. The imaging system

The authors' approach to the measurement challenge used a combination of a Kodak 4540 digital camera, synchronised with an Oxford Lasers LS20 Copper Vapour Laser. The motion of acrylonitrile microspheres within a thick laser light sheet is recorded at a frame rate of 9000 or 13500 frames/s and engine speeds in the range 500–2000 RPM. The laser provides a rapid pulse train of illumination at a rate of one pulse per camera frame. Each individual pulse has a duration of approximately 30 ns and a pulse energy of 3–6 mJ. Selected pairs of successive images in the recorded sequence are interrogated using standard PIV cross-correlation techniques with automated post-processing for velocity data validation. Although the spatial resolution in this work is limited to a sparse grid of approximately 16×16 velocity vectors, a velocity map may be calculated every 1–2° crank angle within a single cycle if required. Depending on the engine speed and camera frame rate, up to nine engine cycles can be captured in a single experiment during a recording time of < 0.7 s. Alternatively, up to the order of 1000 velocity maps at the same engine crank angle can be recorded in a single engine run through appropriate modification of the camera triggering, thus allowing flow statistics to be studied.

The high-speed camera drives the copper vapour laser with a once-per frame synchronisation signal which ensures that each frame corresponds to a single laser pulse. The engine was equipped with both crank and cam encoders to allow selection of the single or repetitive crank angle trigger for the whole system. This ensures that the first image in a sequence corresponds to a known engine crank angle datum. The electronic timing system could also be used to drive a strobe LED in the camera's field of view to identify frames corresponding to each successive TDC engine position. An overview of the system is given in Fig. 1.

The 25 mm diameter beam from the copper vapour laser was formed into a collimated sheet approximately 3 mm thick, using a 1 m focal length positive spherical lens and an 80 mm focal length cylindrical lens, and delivered to the engine using

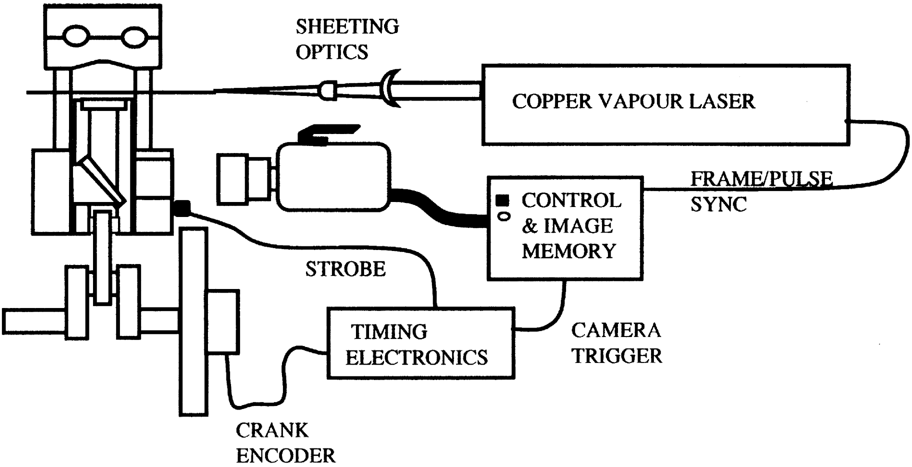

Fig. 1. Schematic of system layout.

Table 1
Camera frame rate and resolution in pixels

Frame rate	Resolution
4500	256 × 256
9000	256 × 128
13 500	128 × 128
18 000	256 × 64
32 000	128 × 64
40 500	64 × 64

a system of mirrors. The potential also exists for fibre delivery of the laser light to a compact sheet generating optical head.

For the results presented here, a camera frame rate and laser repetition rate of 9000 frames/s was used, to enable high axial swirl ratio flows to be investigated at an engine speed of 1500 RPM. The spatial resolution of 256 × 128 pixels at this frame rate allowed a circular region of the flow to be imaged through the engine's fused silica piston crown window, giving a measurement grid of 16 × 16 overlapping regions, at a rate of 1 image per degree CA. The spatial resolution of the Kodak camera as a function of frame rate as shown in Table 1.

When the evolution of the flow over several complete cycles was to be examined, the camera was operated in a free-running condition, triggered by a single TDC marker. This allowed cycle-resolved flow visualisation and flow measurement to be made with a qualitative indication of cyclic variability over a limited number of engine cycles (<10).

For the purpose of quantification of flow variability statistics, many more images are required at a single crank angle. This data may be obtained using the "Random" trigger mode of the Kodak 4540 with successive triggers at the same crank angle on consecutive engine cycles causing 4 frames to be captured at 9000 fps for each individual trigger pulse. For development purposes, data from a sample of 20 engine cycles was deemed suitable, although a much larger data set (up to 1500 image sets can be recorded in memory) would be required for rigorous statistical studies.

2.2. Seeding considerations

Commercially available acrylonitrile microballoons were used as flow seeding. The hollow, thin-shelled particles had a mean diameter of 35 μm and a specific gravity of approximately 0.04. Using the Hjelmfelt/Mockros calculation in [24], a 95% amplitude flow-following accuracy requirement at a 1 kHz flow fluctuation rate in air at standard pressure and temperature yields a limiting particle size of 37 μm. It is worth noting that at the maximum permissible engine speed for the optical engine of 2000 RPM this would correspond to an ability to follow integral length scale vortices rotating at swirl ratios of up to 30. The flow following ability increases as the air density and viscosity increase, i.e. the amplitude-following accuracy improves from the value of 95% as the compression stroke progresses in an IC engine. These particles therefore give improved flow following ability compared to the 40 μm glass microballoons used for in-cylinder LDV by Sanbayashi et al., which followed fluctuations of 250 Hz at a 90% amplitude accuracy [25]. The non-abrasive acrylonitrile spheres used in this work have been used previously in IC engine PIV [26] and flow visualisation studies [27].

An often more stringent requirement of large particles in rotating flows is that their radial velocity due to centrifugal effects be limited to a reasonable percentage (say 2%) of the tangential flow velocity. In a forced vortex, the ratio of the radial to tangential velocities is given by

$$V_r/V_t = \omega_r^2 d_p^2 \rho_p / 18\mu, \tag{1}$$

where ω is the flow's angular rotation rate, d_p is the particle diameter, ρ_p is the particle density and μ is the kinematic viscosity of the fluid [24].

At the maximum engine speed and a swirl ratio of 30 (the maximum we would expect in any IC engine), we could expect to encounter large scale rotation rates of up to 1000 Hz. For the 35 μm diameter particles of specific gravity 0.04 the value of this velocity ratio is approximately 0.002. Centrifugal forces can therefore be neglected within the specified experimental velocity error of $\pm$ 10%. If the kinematic viscosity is increased appropriately for measurements during compression, both the error due to centrifugal force and the flow-following error reduce from the calculated values, so we can safely rely on the flow following characteristics of our seed material for following the large scale flow patterns.

In fact, the roll-off in the frequency response at higher turbulent frequencies acts in favour of the correlation process, since small scale, high magnitude velocity gradients are effectively low-pass filtered by the particle's flow following characteristics. This also gives rise to a spatial and temporal resolution appropriate for comparison with typical CFD data. Furthermore, the particle scattering efficiency is at least two orders of magnitude higher than for the 1–3 μm sized seed particles typically used in high resolution PIV, allowing moderate pulse energies (2–3 mJ) and relatively thick (3 mm) light sheets to be used. This minimises lost particle images due to the out-of-plane velocity component.

For both cycle-resolved and cycle-averaged imaging, a measured quantity of seed was introduced into a large plenum feeding the engine intake and a small through-flow of compressed air allowed to feed the seed/air mixture into the inlet tract. The camera timing system was triggered shortly after the compressed air flow was turned on, and the seed concentration was sufficiently steady to give uniform seed characteristics over several hundred engine cycles.

2.3. Measurement conditions

The engine was a single cylinder four stroke motored optical engine, designed and built by Advanced Engine Technology, Rover Group. The four-valve, four-stroke pent roof chamber engine was equipped with a piston crown and cylinder of fused silica and a "gable end" window providing a view into the pent roof combustion chamber. A schematic of the engine showing optical access for horizontal light sheets is shown in Fig. 2. Measurements in vertical planes could also be made by introducing a light sheet through the glass cylinder and viewing this at a normal through the cylinder wall. The light sheet position for the results presented here is 40 mm down form the cylinder head gasket, or approximately half way down the piston stroke.

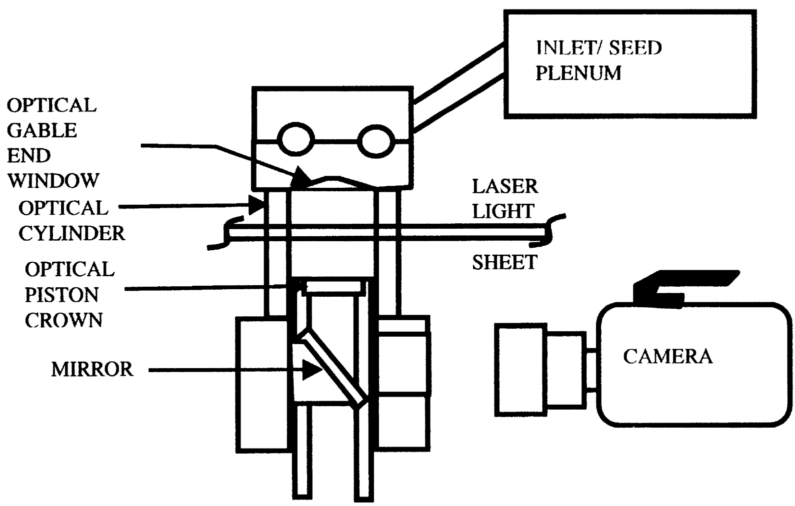

Fig. 2. The single cylinder optical engine showing optical access.

2.4. Image recording: cycle resolved measurements

The high-speed imaging system was used to record the 8-bit flow images at a frame rate of 9000 fps and a resolution of 256 × 128 pixels. A continuous sequence of images was recorded to the camera's control and storage unit for a duration of 0.7 s. Therefore, each recording represented a series of 4–9 engine cycles with a crank-angle resolution of the order of 1°. The LED strobe was fired at TDC of the induction stroke to provide a known crank angle reference for each cycle. The timing diagram for cycle-resolved image acquisition is shown in Fig. 3.

The camera has a built-in feature that allows a single reference frame to be stored and subsequently subtracted from each frame recorded in the image sequence. This provided a convenient means for real-time reduction of image noise due to illumination flare: a single image of the light sheet alone, recorded at a suitable crank angle was used as a reference frame to reduce background self-correlation noise in the cross-correlation between successive particle image fields.

2.5. Image recording: cyclic variability studies

For investigation of cyclic variability, many flow visualisation and PIV results were required at a specific crank angle from successive engine cycles. Using a once per revolution trigger at the specific crank angle to trigger the Kodak control system in "Random" mode, up to 1500 sets of four consecutive frames could be recorded in one engine run. The timing diagram is indicated in Fig. 4.

2.6. Generation of flow visualisation images

Flow visualisation images were generated at each measurement crank angle by adding three successive flow images around the measurement crank angle. This produced pseudo "particle streak" or "particle track" images that were suitable for hard copy presentation and for visual validation of the automatically post-processed PIV data sets. The flow visualisation and velocity data could be conveniently formed into compressed digital video files of moderate size (<1 MB for a sequence of 40 images), giving a powerful means of data reduction for purely visual comparison of flow behaviours between different measurement planes and engine variations.

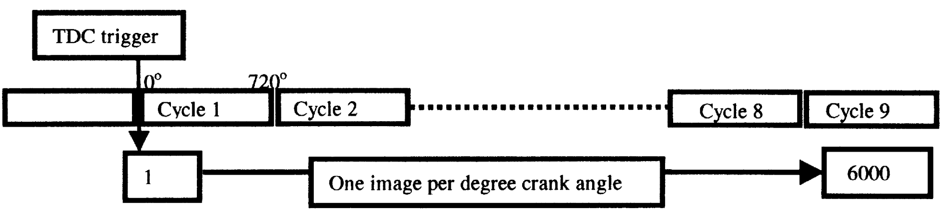

Fig. 3. Image recording scheme for cycle-resolved flow histories.

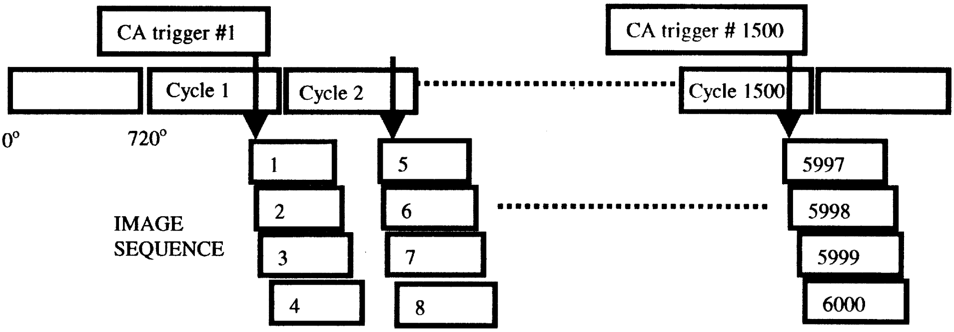

Fig. 4. Image recording scheme for study of cyclic variability at a particular crank angle.

2.7. PIV interrogation

An in-house windows-based software suite for automated cross-correlation of the digital TIF image sequence was developed. This allowed PIV data to be calculated from pairs of successive images at a user-selected crank angle increment within a given engine cycle. Images were interrogated on a square grid with 50% overlap between neighbouring interrogation regions.

Since large numbers of PIV data sets were to be generated, it was essential to maximise data validity rates with a minimum of operator intervention in either the interrogation or post processing stages. For each interrogation region, the image pair were pre-processed with a high pass filter algorithm [23] to mitigate correlations due to common background (low frequency) intensity patterns in the two images. Each of these new images was checked for the presence of particle images using an automatically generated threshold level. If no images were found in either of the image pair, no further processing was performed and the region was excluded from the automated post-processing routines. A standard FFT-based cross-correlation algorithm was employed with the sub-pixel location of the centroids of the four highest signal peaks being recorded. The peak maxima had a resolution of ~ 0.2 pixels, which combined with a maximum displacement limit of 4 pixels, gives a dynamic range of 20. Raw vector maps consisted of vectors derived from the highest signal peak in each region.

The raw vector maps were post-processed using a two stage automated procedure. The first stage aims to select the best-quality vectors from the field using stringent continuity and signal-to-noise ratio checks. Vectors with speeds less than a threshold or greater than a (different) threshold were also eliminated. Secondly, vectors are added iteratively against automatically generated continuity thresholds. Each auto-post-processed vector map is saved to disk. The user then performs manual post-processing on each vector map (typically 20 maps per engine cycle), using the flow visualisation image sequence as a guide. Vector maps corresponding to crank angles after inlet valve closure contain mostly well-ordered flow patterns and required $< 5\%$ of the auto-generated vectors to be modified manually. The vector map sequence was then automatically converted to a bitmap sequence for importing directly into a commercial software package for generation of AVI files.

3. Results and discussion

The techniques discussed here have generated a large database of flow visualisation and measurement data, from engine speeds in the range 500–2000 RPM in a variety of engine configurations. Some illustrative examples of the velocity data and flow visualisation from horizontal planes in a bowl-in-piston axial swirl engine are presented in the following pages. The results in Figs. 5 and 6 correspond to an engine crank speed of 700 RPM and a camera frame rate of 9000 frames/s. Thus, the available crank angle resolution is better than 1°CA in this case. The field of view permitted by the piston crown window is a circle approximately 70 mm in diameter, giving a measurement grid of ~ 5 mm. The smallest vortex that can be resolved clearly at this resolution is the order of 10 mm in diameter.

The flow visualisation "streak" images to the left and the PIV maps to the right are accompanied by a small schematic of the engine cross-section showing the instantaneous crank angle and the relative positions of the piston and light sheet (single horizontal dotted line). In each case the images are separated by 10° of crank angle rotation. In the AVI movie versions, these diagrams are animated to give an impression of the engine crank angle and the position of the piston top relative to the sheet, to aid interpretation of the results. Some caution is required in interpreting the flow visualisation images in the sense that short streaks may indicate either a low in-plane velocity or movement of the particle out of the light sheet. However, the flow visualisation is a useful cross-check of the PIV data maps and provides visualisation to finer flow scales than the PIV vector data.

Fig. 5 shows flow visualisation and velocity vector maps from six crank angles around the crank angle of inlet valve closure, from 160 to 210° after TDC. This corresponds to the piston moving only a short distance down towards BDC and then up into the start of the compression stroke. Although the piston movement is only very slight during this period, the swirl centre is shown to drift considerably with significant changes in flow pattern from one crank angle interval to the next. Fig. 6 shows a sequence of six crank angles after the time of inlet valve closure, 240–290°CA after TDC. These show a continuing drift of the swirl centre, followed by a strong modification of the flow as the piston approaches the light sheet plane (270–290°CA). The evolution of the flow can clearly be seen in the flow visualisation and PIV vector maps.

The PIV vector maps show that the flow is not a simple solid body rotation. Large spatial variations in the in-plane velocity indicate either a significant deviation from

Fig. 5. Cycle resolved flow visualisation and PIV data at 10°CA intervals about inlet valve closure. Engine speed 700 RPM.

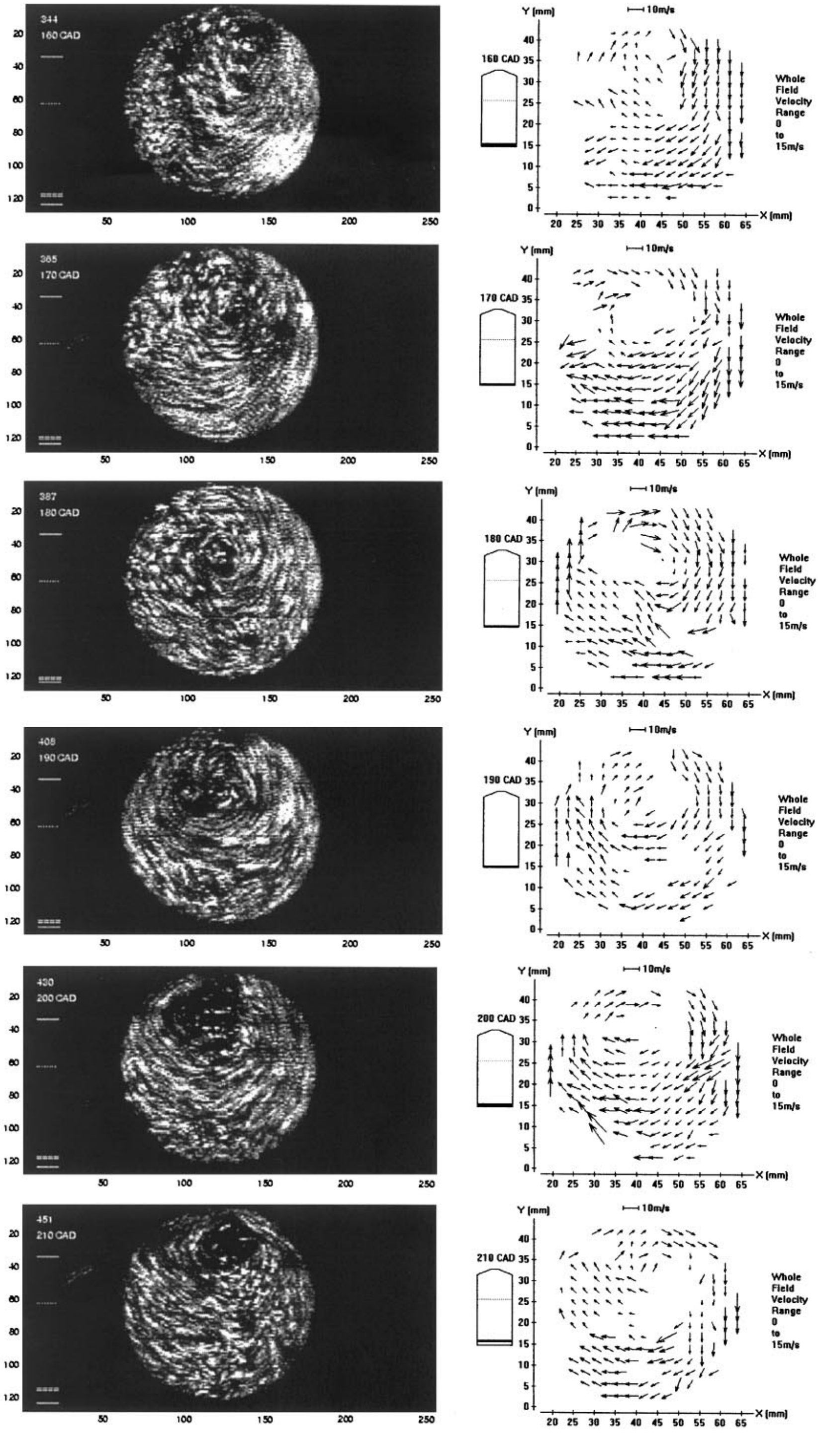
344
160 CAD
385
170 CAD
387
180 CAD
408
190 CAD
430
200 CAD
451
210 CAD
Y (mm)
X (mm)
10m/s
160 CAD
170 CAD
180 CAD
190 CAD
200 CAD
210 CAD
Whole Field Velocity Range 0 to 15m/s

whole-body rotation or a significant out-of-plane velocity structure. Similar observations have been made in strong tumbling flows, where much of the flow momentum was contained in a swirl "tongue" that precessed around the cylinder volume [12,15]. The results here confirm that the detailed *temporal* and *spatial* structure of the flow must be considered when optimising fluid mechanical design for particular combustion strategies.

4. Conclusions

The use of electronic high-speed imaging in combination with a pulsed copper vapour laser strobe is providing a convenient and powerful tool for the rapid characterisation of in-cylinder flow in the context of an industrial engine development need. The use of a turnkey laser and camera system, relatively thick light sheets, real-time imaging and the potential for full fibre-optic light sheet delivery provide important benefits in terms of experimental simplicity and safety.

The pseudo-streak flow visualisation enables the salient evolving flow features to be captured and presented in hard copy format (or AVI video) with valuable benefits in data reduction, report generation and ease of comparison of different engine designs. The cyclically resolved PIV data, while of reduced accuracy and spatial resolution compared with photographic or high-resolution digital recording, provides suitable quantification of major flow characteristics on a timescale appropriate to engine development. The ability to present the flow visualisation and velocity data in the forms of printed hard-copy and digital video (AVI) form enables rapid and convenient comparison of engine variants and has proved a major benefit in this work. This technique has been found to provide a powerful complement to the high resolution, two-colour photographic PIV "snapshots" reported previously [28] by the same group.

Future possibilities for the technique include cycle-resolved correlation of flow and performance parameters, and conditional data recording to determine the effect of flow behaviour on abnormal combustion events.

Acknowledgements

The authors would like to thank Dr Mitch Patrie and Bill Church (formerly at the University of Wisconsin-Madison's Engine Research Centre), for their kind advice and assistance, and Dr Andrew Moore of Heriot-Watt University for valuable discussions. The optical engine was designed and supplied by Advanced Engine Technology, Rover Group.

Fig. 6. Cycle resolved flow visualisation and PIV data at 10°CA intervals during the compression stroke. Engine speed 700 RPM, high axial swirl condition.

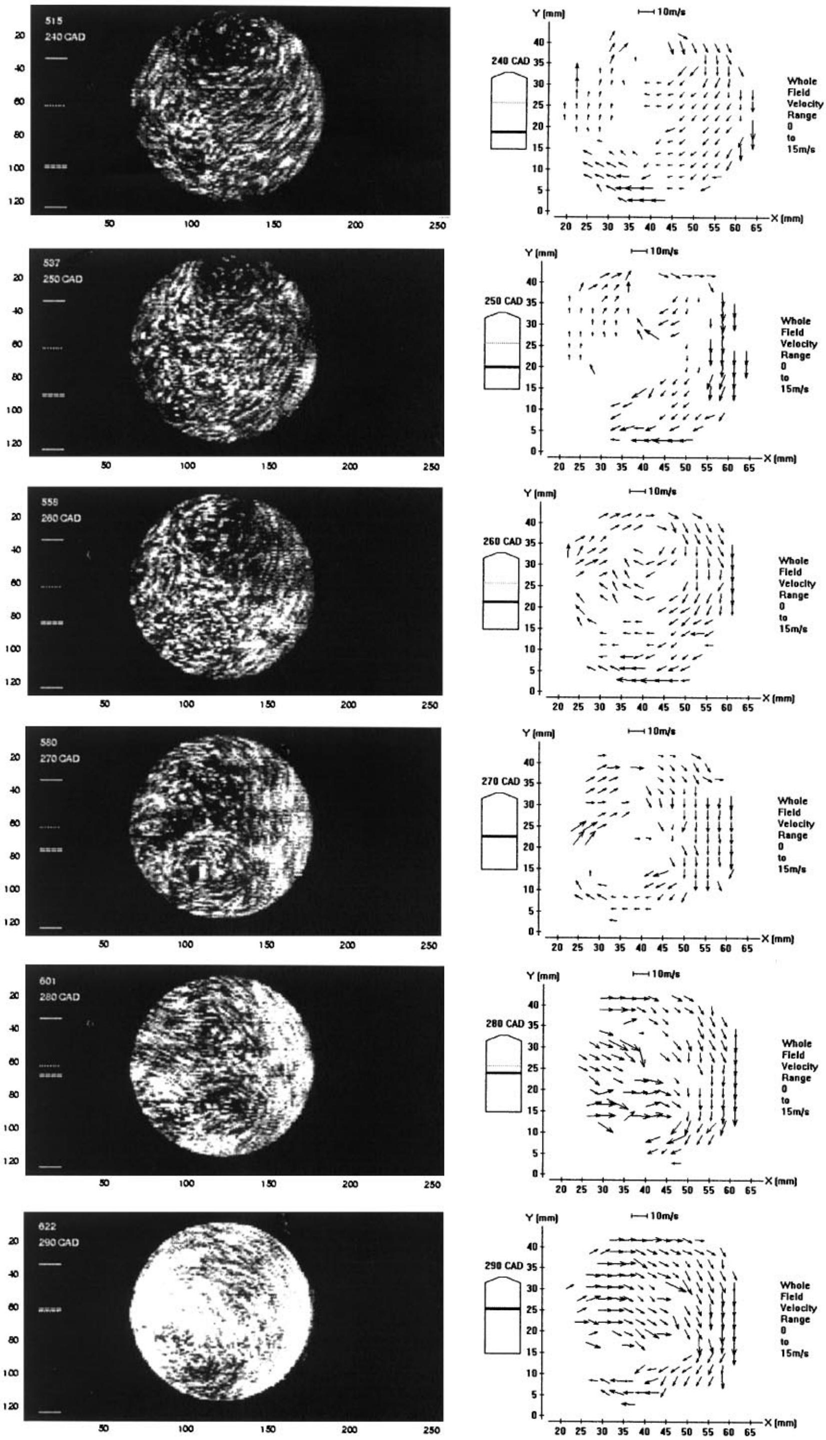
515
240 CAD
537
250 CAD
558
260 CAD
580
270 CAD
601
280 CAD
622
290 CAD
Y (mm)
X (mm)
10m/s
240 CAD
250 CAD
260 CAD
270 CAD
280 CAD
290 CAD
Whole Field Velocity Range 0 to 15m/s

References

[1] Arcoumanis C, Whitelaw JH. Fluid Mechanics of Internal Combustion Engines—a Review. Proc Instn Mech Engrs 1987;201:C1.
[2] Heywood JB. Fluid motion within the cylinder of internal combustion engines—The 1986 Freeman Scholar Lecture. Trans ASME J Fluids Eng 1987:109.
[3] Khaligi B. Intake-generated swirl and tumble motions in a 4-valve engine with various intake configurations-flow visualisation and particle tracking velocimetry. SAE Congress and Exp, Detroit, 1990; paper # 900059.
[4] Ronnback M, Le WX, Linna JR. Study of induction tumble by particle tracking velocimetry in a 4-valve engine. Trans SAE 1991; paper # 912376.
[5] Rimai L, Adamczyk AA, Mikulec A, Kent JC. Quantitative three-dimensional reconstruction of flow fields from orthogonal views of particle tracks: application to a water analog of a piston engine. In: Proceedings of the 5th International Symposium on Flow Visualisation, Prague, Hungary, 1989.
[6] Reuss DL, Adrian RJ, Landreth CC, French, DT, Fansler, TD. Instantaneous planar measurements of velocity and large-scale vorticity and strain rate in an engine using particle image velocimetry. SAE Congress and Exp, Detroit, 1989; paper # 890616.
[7] Reeves M, Garner CP, Dent JC, Halliwell NA. Study of barrel swirl in a four-valve optical IC engine using particle image velocimetry. COMODIA 94 Conference on Combustion Diagnostics and Modelling in IC engines, Yokohama, Japan, July 1994.
[8] Adrian RJ. Particle imaging techniques for experimental fluid mechanics. Ann Rev Fluid Mech 1991;23:261–304.
[9] Reuss DL, Bardsley M, Felton PG, Landreth CC, Adrian RJ. Velocity, vorticity, and strain rate ahead of a flame measured in an engine using particle image velocimetry. SAE Congress and Exp, Detroit, 1990; paper # 900053.
[10] Lee J, Farrell PV. Intake valve flow measurements of an IC engine using particle image velocimetry. SAE Congress and Exp, Detroit, 1993; paper # 930480.
[11] Nino E, Gajdeczko BF, Felton PG. Two-colour particle image velocimetry in an engine with combustion. SAE Congress and Exp, Detroit, 1993; SAE paper # 930872.
[12] Reeves M, Haste MJ, Garner CP, Halliwell NA. Barrel swirl breakdown in SI engines: insights from particle image velocimetry measurements. Accepted for publication in I Mech E Part D: J Automobile Eng 1999.
[13] Adrian RJ. Dynamic ranges of velocity and spatial resolution of particle image velocimetry. Meas Sci Tech 1997;8(12):1393–8.
[14] Reuss DL, Rosalik ME. PIV measurements during combustion in a reciprocating internal combustion engine. International Conference on Application of Laser Techniques to Fluid Mechanics, Lisbon, Portugal, vol. 37, 1998. p. 1.1–1.17.
[15] Reeves M. Particle image velocimetry applied to internal combustion engine in-cylinder flows. Ph.D. Thesis, Loughborough University of Technology, England, September 1995.
[16] Rouland E, Trinite M, Dionnet F, Floch A, Ahmed A. Particle image velocimetrty mesaurements in a high tumble engine for in-cylinder flow structure analysis. SAE Congress and Exp, Detroit, 1997; paper # 972831.
[17] Brucker Ch. 3D scanning PIV applied to an air flow in a motored engine using digital high speed video. Meas Sci Tech 1997;8(12):1481–92.
[18] Hinsch KD. Particle image velocimetry. In: Rajpal S, Sirohi, editor. Speckle metrology, New York: Marcel Dekker Inc., 1993.
[19] Keane RD, Adrian RJ. Theory of cross-correlation analysis of PIV images. J Appl Sci Res 1992;49:191–215.
[20] Lecordier B, Mouqallid M, Trinite M. Simultaneous 2D measurements of flame front propagation by high-speed tomography and velocity field by cross correlation. In: Proceedings of the 8th International Symposium on Application of Laser Techniques to Fluid Mechanics Lisbon, Portugal, July 1994.

[21] Stolz W, Kohler J, Lawrenz W, Meier F, Bloss WH, Maly RR, Herweg R, Zahn M. Cycle resolved flow field measurements using a PIV movie technique in a SI engine. SAE International Fuels and Lubricants Meeting and Exposition, San Francisco, October 1992; Paper # 922354.
[22] Wormell DC, Sopchak JL. A particle image velocimetry system using a high resolution CCD camera. Conference on Optical methods and Data Processing in Heat and Fluid Flow, City University, London, UK, April 1994; IMechE C485/014.
[23] Willert C. Stereoscopic digital particle image velocimetry for application in wind tunnel flows. Meas Sci Tech 1997;8(12):1465–79.
[24] Melling A. Tracer particles and seeding for particle image velocimetry. Meas Sci Tech 1997;8(12):1406–16.
[25] Sanbayashi D, Ando H, Kumagai H. Feasibility of using several power materials as the seeding particle for LDV measurement. JSAE Rev 1991;12(2).
[26] Patrie MP, Martin JK. PIV measurements of in-cylinder flow structures and correlation with engine performance. In: Proceedings of the ASME Internal Combustion Engine Division 19th Annual Fall Technical Conference, 1997; paper # 97-ICE-73.
[27] Merzkirch W. Flow visualisation. 2nd ed. New York: Academic Press, 1987.
[28] Towers DP, Buckberry CH, Reeves M. Development of a 2 colour PIV system for in-cylinder spark ignition engine flows. In: Ninth International Symposium on Application of Laser Technologies to Fluid Mechanics Lisbon, Portugal, 1998; Session Engines—I.